

Structural, Spectroscopic, and Electrochemical Characterization of Tetrakis- μ -(2-pyrrolidinonato)-dirhodium(II) and Tetrakis- μ -(δ -valerolactamato)-dirhodium(II) †

John L. Bear,* Robert S. Lifsey, Lai K. Chau, Mohammad Q. Ahsan, James D. Korp, Madhav Chavan, and Karl M. Kadish*

Department of Chemistry, University of Houston, Houston, Texas 77044, U.S.A.

The structure, chemical properties, and electrochemistry of two tetralactamato bridged dirhodium(II) complexes is reported. These complexes were formed by a ligand-exchange reaction involving 2-pyrrolidinone (Hpyro) and δ -valerolactam (Hvall) (2-piperidinone) with the acetate groups of $[\text{Rh}_2(\text{O}_2\text{CCH}_3)_4]$. Compound $[\text{Rh}_2(\text{pyro})_4(\text{Hpyro})_2] \cdot 2\text{CH}_2\text{Cl}_2$ (**1a**) crystallizes in space group $P\bar{1}$ (triclinic) with cell constants $a = 9.186(1)$, $b = 9.569(1)$, $c = 10.458(1)$ Å, $\alpha = 107.28(1)$, $\beta = 99.15(1)$, $\gamma = 95.07(1)^\circ$, and $Z = 1$. The structure refinement converged to $R = 0.032$ and $R' = 0.038$. Compound $[\text{Rh}_2(\text{vall})_4(\text{Hvall})_2] \cdot 2\text{Hvall}$ (**2a**) crystallizes in the monoclinic space group $C2/c$ with cell constants $a = 19.990(3)$, $b = 10.567(1)$, $c = 21.784(7)$ Å, $\beta = 99.47(2)^\circ$, and $Z = 4$. The sample decayed rapidly, which limited the amount of available data, but the refined model converged at $R = 0.035$ indicating good accuracy. The prominent feature common to compounds (**1a**) and (**2a**) is the 'cis' arrangement of the bridging ions, where two cis nitrogens and two cis oxygens are bound to each Rh ion. The Rh–Rh bond lengths are 2.445(1) and 2.392(1) Å, respectively. The oxidation potentials for $[\text{Rh}_2(\text{pyro})_4]$ (**1**) and $[\text{Rh}_2(\text{vall})_4]$ (**2**) in CH_3CN are +0.15 and +0.04 V vs. s.c.e. Carbon monoxide binding to (**1**) and (**2**) is rapid and reversible in binding solvents such as CH_3CN . However, in non-bonding solvents CO adduct formation is fast but CO dissociation is very slow. Formation constants for CO binding to (**1**) and (**2**) in CH_3CN were $\log(K_{\text{CO}}/\text{atm}^{-1}) = 1.63 \pm 0.05$ and 2.11 ± 0.06 , respectively.

It has been shown that dirhodium(II) acetamidate complexes form stable adducts with carbon monoxide even in bonding solvents such as acetonitrile and water, whereas CO addition to dirhodium(II) carboxylates is quite weak and only occurs in non-bonding solvents.¹ In all cases, CO bonding was found to be rapid and reversible. We recently reported that the CO adduct of $[\text{Rh}_2(\text{tcl})_4]$ [$\text{tcl} = -\text{NC}(\text{S})(\text{CH}_2)_4\text{CH}_2(\omega\text{-thiocaprolactamate})$] is even more stable than the tetrakis(acetamidate) complex.^{2a} The compound $[\text{Rh}_2(\text{tcl})_4]$ is different from carboxylate or amidate bridged complexes in several respects. This complex, which was prepared by reacting $[\text{Rh}_2(\text{O}_2\text{CCH}_3)_4]$ in a melt of ω -thiocaprolactam, has four sulphurs bound to one rhodium and four nitrogens bound to the second rhodium ion. $[\text{Rh}_2(\text{tcl})_4]$ also forms only mono adducts and reacts irreversibly with CO to form $[\text{Rh}_2(\text{tcl})_4(\text{CO})]$ which is stable in boiling acetonitrile for several hours.

The unusual chemistry and polar nature of $[\text{Rh}_2(\text{tcl})_4]$ raises questions with respect to lactam-bridged dirhodium complexes in general. For example, does the polar geometry of $[\text{Rh}_2(\text{tcl})_4]$ result from structural properties of the lactam (steric factors) or the presence of the sulphur donor (electronic factors)? The same question can be asked regarding the thermodynamics and kinetics of axial ligand exchange. Since no other lactam complexes of dirhodium(II) have been reported, we have synthesized the five- and six-membered ring lactam complexes. This paper reports the molecular structure, electrochemical properties, and CO binding properties of tetrakis- μ -(2-pyrrolidinonato)-dirhodium(II) and tetrakis- μ -(δ -valerolactamato)-dirhodium(II).

Experimental

Chemicals.—Rhodium(II) acetate was purchased from Matthey Bishop Inc. The ligands, 2-pyrrolidinone (Hpyro) and δ -valerolactam (Hvall) (2-piperidinone), were obtained from the Aldrich Chemical Co. and recrystallized from CH_2Cl_2 prior to use. All solvents used were reagent grade and distilled over CaH_2 or P_2O_5 and stored over molecular sieves prior to use. Acetone was purified by adding successive small amounts of potassium permanganate at reflux until the violet colour persisted. This was followed by distillation and drying over 4 Å molecular sieves. The supporting electrolyte, tetrabutylammonium perchlorate, was recrystallized from ethanol and vacuum oven dried prior to use.

Synthesis of $[\text{Rh}_2(\text{pyro})_4]$ (1**).**—A mixture of 2-pyrrolidinone (5.0 g, 59 mmol) and $[\text{Rh}_2(\text{O}_2\text{CCH}_3)_4]$ (0.20 g, 0.45 mmol) was placed in an evacuated 25-cm³ round-bottomed flask. The mixture was heated at 125 °C and magnetically stirred for 20 h. Most of the excess ligand was removed by sublimation. The reaction mixture was then dissolved in CH_2Cl_2 and upon evaporation, large reddish purple crystals were deposited. One of these crystals was selected for X-ray structure determination. The solid was removed by filtration and dissolved in CH_3OH for purification using h.p.l.c.^{2b} This procedure was used to remove axially bound 2-pyrrolidinone through displacement on the CN-bonded phase column and to separate the different substitution products. The major product was the totally substituted complex (ca. 90%). Methanol was removed on a Rotovap to give a blue solid. When the solid was dried in a vacuum oven the axially bound methanol was lost and the solid became light green.

Synthesis of $[\text{Rh}_2(\text{vall})_4]$ (2**).**—The same procedure outlined above was used to synthesize $[\text{Rh}_2(\text{vall})_4]$. However, the

† Supplementary data available: see Instructions for Authors, *J. Chem. Soc., Dalton Trans.*, 1989, Issue 1, pp. xvii–xx.

Non-S.I. unit employed: atm = 101 325 Pa.

exchange reaction with valerolactam was much slower. Samples were taken from the reaction mixture every 12 h and separated on the liquid chromatograph to determine the ratio of substitution products. The reaction required 96 h at 125 °C to produce a significant amount of the totally substituted complex (ca. 50%). The remaining 50% of product was $[\text{Rh}_2(\text{vall})_3(\text{O}_2\text{CCH}_3)]$.

Instrumentation.—A Waters Associates h.p.l.c. system was used in the separation procedure. The system consisted of a model 6000A solvent delivery system, a model U6-K injector, a model 440 variable wavelength detector, and an RCM-100 radial compression module containing a 10- μm Radial-Pak CN column. The mobile phase was high purity h.p.l.c. methanol. An EG&G, Princeton Applied Research model 174A/175 polarograph potentiostat system or an IBM EC 225 voltammetric analyzer was used for electrochemical measurements. A three-electrode system was utilized consisting of a platinum button working electrode, a platinum wire auxiliary electrode, and a saturated calomel electrode (s.c.e.). All potentials are referenced versus s.c.e. E.s.r. spectra were recorded on an IBM model ER 100E e.s.r. spectrometer.

Gas mixtures containing different proportions of CO and Ar were prepared using Matheson Dyna Blenders model 8250 electronic gas flow meters/controllers. The total gas pressure was assumed to be 1 atm and the ratio of CO flow rate to total flow rate was assumed to be the partial pressure of CO. These gas mixtures were passed through a bubbler containing the particular solvent for ca. 5 min before passing the gas through the sample solution for exactly 2 min. An IBM 9430 u.v.-visible spectrophotometer was used to record electronic absorption spectra of the neutral complexes.

Calculation of CO Binding Constants.—The Ketelaar equation was used to calculate formation constants of the monocarbonyl adducts. Details on this calculation are given in ref. 1. Values of K_{CO} were initially calculated from a linear least-squares analysis of $1/(A - A_0)$ vs. $1/p_{\text{CO}}$. These initial K_{CO} values were then used as estimates of K_{CO} in order to calculate more refined values of the binding constants. This was done using a non-linear least-squares program. Calculations were carried out at three different wavelengths and an average value of the binding constant is reported.

X-Ray Structure Determination of $[\text{Rh}_2(\text{pyro})_4(\text{Hpyro})_2] \cdot 2\text{CH}_2\text{Cl}_2$ (1a).—Details of data collection and refinement are given in Table 1. The crystals were observed to decompose within ca. 2 h when removed from the mother-liquor, and for this reason the sample was coated with epoxy resin in order to retard loss of crystallization solvent. Two standard reflections were monitored periodically during the course of the data collection, and showed a 4.5% decay over the 43 h of the experiment. A linear decay correction was made in order to account for this. No correction for absorption was made due to the small absorption coefficient. The structure was solved by the Patterson method, and revealed the position of the unique Rh atom in the asymmetric unit, which is comprised of one-half molecule situated about an inversion centre at $(0, \frac{1}{2}, \frac{1}{2})$. A methylene chloride solvent molecule was found located in channels parallel to the *b* axis which accounts for the rapid decomposition of the crystals mentioned above. All hydrogens were entered in ideal calculated positions, except for H(1) [bonded to N(3)], which was found in a difference map and refined independently. Hydrogen thermal parameters were estimated based on the thermal motion of the associated carbons. Convergence was reached at the agreement factors listed in Table 1 after all shift/deviation ratios were less than 0.1. No unusually high correlations were noted between any of

Table 1. Data collection and processing parameters^a for $[\text{Rh}_2(\text{pyro})_4(\text{Hpyro})_2] \cdot 2\text{CH}_2\text{Cl}_2$ (1a) and $[\text{Rh}_2(\text{vall})_4(\text{Hvall})_2] \cdot 2\text{Hvall}$ (2a)

Compound	(1a)	(2a)
Colour	Reddish purple	Crimson
Sample size/mm	0.60 × 0.40 × 0.30	0.50 × 0.50 × 0.40
Diffractometer	Nonius CAD4	Nonius CAD4
Space group	<i>P</i> $\bar{1}$, triclinic	<i>C</i> 2/ <i>c</i> , monoclinic
<i>a</i> /Å	9.186(1)	19.990(3)
<i>b</i> /Å	9.569(1)	10.567(1)
<i>c</i> /Å	10.458(1)	21.784(7)
α /°	107.28(1)	
β /°	99.15(1)	99.47(2)
γ /°	95.07(1)	
<i>U</i> /Å ³	857.6	4 538
Formula	$\text{C}_{24}\text{H}_{38}\text{N}_6\text{O}_6\text{Rh}_2 \cdot 2\text{CH}_2\text{Cl}_2$	$\text{C}_{40}\text{H}_{68}\text{N}_8\text{O}_8\text{Rh}_2$
<i>M</i>	882.3	994.9
<i>Z</i>	1	4
<i>D</i> _c /g cm ⁻³	1.71	1.46
$\mu(\text{Mo-K}\alpha)/\text{cm}^{-1}$	13.08	7.70
2 θ range/°	4 < 2 θ < 50	4 < 2 θ < 40
Scan width ($\Delta\theta$)/°	0.9 + 0.35 tan θ	0.9 + 0.35 tan θ
Max. scan time/s	60	120
Scan speed range/° min ⁻¹	1.3—6.7	0.7—5.0
Scan method	θ —2 θ	θ —2 θ
Total data collected	3 014	1 392
Independent data,	2 568	1 159
<i>I</i> > 3 σ (<i>I</i>)		
Total variables	203	270
<i>R</i> ^b	0.032	0.035
<i>R</i> ' ^b	0.038	0.039

^a Radiation = Mo-K α , $\lambda = 0.710 73$ Å. ^b $R = \Sigma|F_o| - |F_c| / \Sigma|F_o|$ and $R' = [\Sigma w(|F_o| - |F_c|)^2 / \Sigma w|F_o|^2]^{1/2}$ with weights $w = \sigma_F^{-2}$.

the variables in the last cycle of least-squares refinement, and the final difference-density map showed no peaks greater than 0.70 e Å⁻³, which is near the Rh atom. All calculations were made using Molecular Structure Corp.'s TEXRAY 230 modifications of the SDP-PLUS series of programs.

X-Ray Structure Determination of $[\text{Rh}_2(\text{vall})_4(\text{Hvall})_2] \cdot 2\text{Hvall}$ (2a).—Details are listed in Table 1. The two standard reflections showed a 30% decay over the 2 d of data collection, and a linear decay correction was applied to account for this. No correction for absorption was made due to the small absorption coefficient. The structure was solved by the Patterson technique, and revealed the position of the single Rh atom in the asymmetric unit, which comprises only one-half molecule situated about a two-fold axis. All hydrogens were entered ideally except for H(3) [bonded to N(3)] and H(4) [bonded to N(4)], which were located in difference maps and refined. Convergence was reached after all shift/deviation ratios were less than 0.3. No unusually high correlations were noted between any of the variables in the last cycle of least-squares refinement and the final difference-density map showed no peaks greater than 0.20 e Å⁻³.

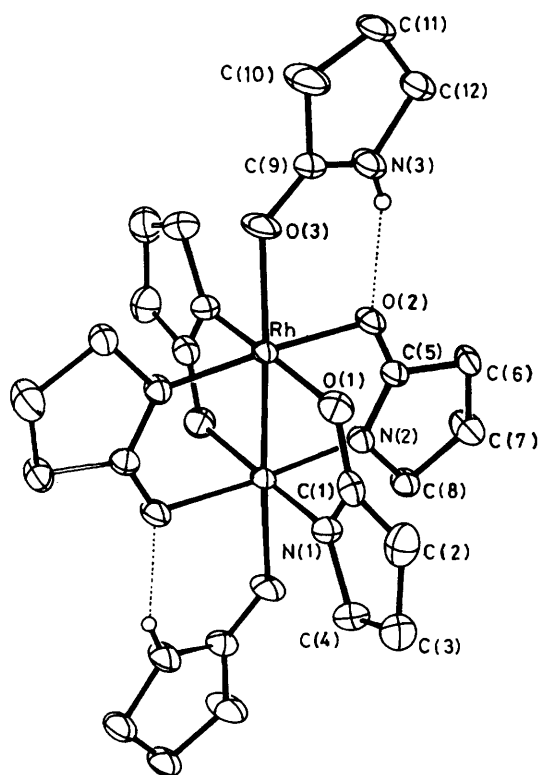
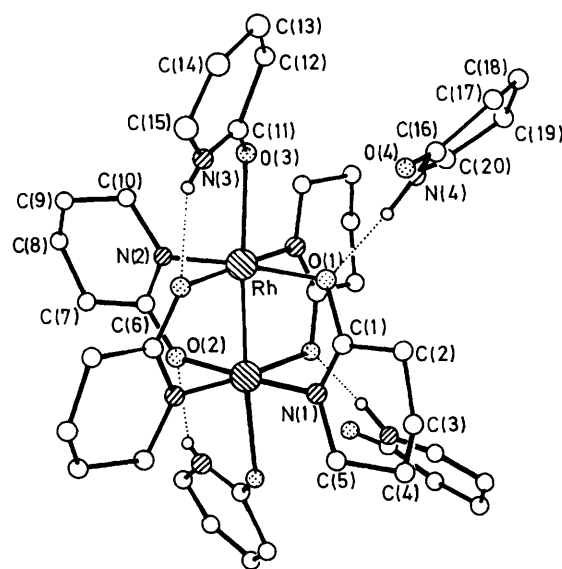
Additional material available from the Cambridge Crystallographic Data Centre comprises thermal parameters, remaining bond lengths and angles, and torsion angles.

Results and Discussion

Crystal and Molecular Structures.—The structures of $[\text{Rh}_2(\text{pyro})_4(\text{Hpyro})_2] \cdot 2\text{CH}_2\text{Cl}_2$ (1a) and $[\text{Rh}_2(\text{vall})_4(\text{Hvall})_2] \cdot 2\text{Hvall}$ (2a) are shown in Figures 1 and 2, respectively. Both complexes have the same geometric arrangement of bridging

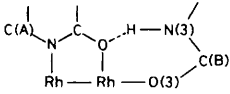
Table 2. Positional parameters and their estimated standard deviations for $[\text{Rh}_2(\text{pyro})_4(\text{Hpyro})_2] \cdot 2\text{CH}_2\text{Cl}_2$ (**1a**) and $[\text{Rh}_2(\text{vall})_4(\text{Hvall})_2] \cdot 2\text{Hvall}$ (**2a**)

(1a)				(2a)			
Atom	x	y	z	Atom	x	y	z
Rh	0.002 87(4)	0.420 19(3)	0.385 21(3)	Rh	0.048 25(5)	0.045 53(6)	0.223 99(3)
Cl(1)	0.394 2(3)	0.790 2(2)	0.113 9(2)	O(1)	0.004 3(3)	0.193 4(5)	0.169 5(2)
Cl(2)	0.517 6(2)	0.809 9(3)	-0.118 1(2)	O(2)	-0.000 1(4)	-0.083 6(5)	0.338 2(2)
O(1)	-0.197 4(3)	0.479 1(3)	0.311 2(3)	O(3)	0.139 0(4)	0.060 3(5)	0.167 6(2)
O(2)	0.115 4(3)	0.597 8(3)	0.346 7(3)	O(4)	0.538 8(4)	0.193 9(7)	0.510 1(3)
O(3)	-0.001 9(4)	0.258 8(3)	0.168 4(3)	N(1)	-0.093 4(4)	0.167 9(6)	0.211 4(3)
N(1)	-0.197 8(4)	0.622 0(4)	0.530 6(3)	N(2)	0.084 7(4)	-0.102 4(6)	0.279 1(3)
N(2)	0.104 6(4)	0.739 4(3)	0.562 8(3)	N(3)	0.090 6(4)	-0.036 6(8)	0.079 4(3)
N(3)	0.144 0(5)	0.409 6(4)	0.092 0(3)	N(4)	0.579 7(5)	0.138 6(7)	0.605 8(3)
C(1)	-0.256 5(5)	0.566 1(4)	0.401 2(4)	C(1)	-0.060 1(5)	0.215 8(7)	0.171 9(4)
C(2)	-0.404 7(6)	0.613 8(5)	0.363 6(5)	C(2)	-0.088 9(5)	0.312 6(7)	0.121 8(4)
C(3)	-0.435 4(6)	0.705 8(6)	0.499 7(5)	C(3)	-0.165 0(6)	0.316 4(8)	0.112 1(4)
C(4)	-0.294 5(6)	0.714 7(6)	0.604 1(5)	C(4)	-0.191 2(6)	0.311 5(9)	0.172 0(4)
C(5)	0.139 5(5)	0.719 5(4)	0.443 7(4)	C(5)	-0.164 2(6)	0.195 3(8)	0.207 8(4)
C(6)	0.211 4(5)	0.860 7(4)	0.428 3(4)	C(6)	0.052 2(5)	-0.139 7(8)	0.323 6(3)
C(7)	0.231 4(6)	0.970 6(5)	0.570 1(5)	C(7)	0.074 0(6)	-0.257 9(8)	0.361 3(4)
C(8)	0.141 0(6)	0.894 2(5)	0.647 9(4)	C(8)	0.140 1(6)	-0.310 1(1)	0.351 8(6)
C(9)	0.061 1(5)	0.285 4(5)	0.080 2(4)	C(9)	0.158 2(8)	-0.293 1(1)	0.294 3(5)
C(10)	0.054 4(7)	0.179 6(6)	-0.059 3(5)	C(10)	0.142 8(5)	-0.168 3(8)	0.261 7(4)
C(11)	0.148 4(6)	0.257 6(6)	-0.126 6(4)	C(11)	0.135 5(6)	0.036 2(8)	0.111 0(4)
C(12)	0.200 8(6)	0.411 8(5)	-0.028 8(4)	C(12)	0.191 2(6)	0.090 8(8)	0.078 9(4)
C(13)	0.355 6(7)	0.793 8(7)	-0.053 9(5)	C(13)	0.182 3(7)	0.067 1(1)	0.011 2(5)
				C(14)	0.131 9(8)	-0.013 1(1)	-0.014 9(4)
				C(15)	0.087 3(7)	-0.072 1(1)	0.014 2(4)
				C(16)	0.571 7(5)	0.122 2(9)	0.545 6(4)
				C(17)	0.607 8(7)	0.017 1(1)	0.520 9(5)
				C(18)	0.652 7(8)	-0.057 1(1)	0.568 6(6)
				C(19)	0.644 5(7)	-0.049 1(1)	0.625 9(6)
				C(20)	0.618 0(6)	0.060 1(1)	0.653 0(4)

**Figure 1.** Labeled ORTEP diagram of $[\text{Rh}_2(\text{pyro})_4(\text{Hpyro})_2] \cdot 2\text{CH}_2\text{Cl}_2$ (**1a**)**Figure 2.** Labeled ORTEP diagram of $[\text{Rh}_2(\text{vall})_4(\text{Hvall})_2] \cdot 2\text{Hvall}$ (**2a**)

ligands, where each rhodium is bound to two *cis* nitrogens and two *cis* oxygens. This is identical to the arrangement found for $[\text{Rh}_2(\text{HNCOCF}_3)_4]$,³ $[\text{Rh}_2(\text{HNCOCH}_3)_4]$,⁴ and one isomer of $[\text{Rh}_2(\text{PhNCOCH}_3)_4]$.⁵ Both compounds also have two lactam ligands bound through the oxygen donor atoms at each axial site, stabilized by intramolecular hydrogen bonds. The positional parameters and selected bond lengths and angles are given in Tables 2 and 3, respectively.

Table 3. Average bond lengths (Å) and angles (°) for $[\text{Rh}_2(\text{pyro})_4(\text{Hpyro})_2] \cdot 2\text{CH}_2\text{Cl}_2$ (**1a**) and $[\text{Rh}_2(\text{vall})_4(\text{Hvall})_2] \cdot 2\text{Hvall}$ (**2a**)



	(1a)	(2a)
Rh-Rh	2.445(1)	2.392(1)
Rh-N	1.998(2)	2.022(3)
Rh-O	2.078(1)	2.059(4)
Rh-O(3)	2.325(1)	2.357(3)
N-C	1.301(3)	1.295(7)
O-C	1.278(2)	1.303(8)
N(3)-C(B)	1.315(3)	1.291(7)
O(3)-C(B)	1.238(2)	1.250(5)
N-C(A)	1.458(3)	1.445(7)
O...H	2.07(2)	2.14
Rh-Rh-O	89.94(4)	88.9(2)
Rh-Rh-N	85.63(4)	88.1(2)
Rh-Rh-O(3)	176.76(4)	175.06(7)
Rh-O-C	115.4(1)	116.5(5)
Rh-N-C	124.5(2)	119.9(5)
Rh-O(3)-C(B)	126.2(1)	125.3(4)
N-Rh-N'	90.28(7)	90.3(2)
N-Rh-O'	90.08(6)	89.4(2)
O-Rh-O'	89.21(6)	90.8(2)
O-C-N	125.5(2)	124.9(7)
O(3)-C(B)-N(3)	126.5(2)	124.6(7)
N-Rh-Rh-O	0.9(2)	8.9(7)

As seen in Table 3, the Rh-Rh bond distance for compound (**1a**) is 0.053 Å longer than that for compound (**2a**). The magnitude of the difference is surprising considering the similarity of the bridging and axial ligands. The O-C-N bond angle of the axial lactam of (**1a**) is larger than that for (**2a**), but the difference is insignificant for the bridging ligands. A model of the two complexes shows that the axial positions of (**2a**) are more sterically hindered by the $-\text{CH}_2-$ groups bound to the lactam nitrogens of the bridging ligands, which may result in the greater torsional twist of the two equatorial rhodium planes observed for (**2a**). Steric crowding is also reflected in a longer Rh-O axial bond and is probably the reason for the shorter Rh-Rh bond length for (**2a**).

Compound (**2a**) crystallized with three different modes of valerolactam ligand interactions and thus offers a good model for evaluating the effect these interactions have on the bond distances and angles of the complex. One type of interaction involves only hydrogen bonding through N-H. The second type involves axial bonding through oxygen and hydrogen bonding through N-H. Finally, there is a bridging interaction (combined with the above hydrogen bonding) for all four equatorial ligands. The N-C-O angles are 121.8(5), 124.6(7), and 124.9(7)°, respectively. Clearly there is an increase in the angle with a direct Rh-ligand bond, but there is no significant difference between the angles of the bridging and the axial ligands. For the three types of interaction a relatively large effect is observed in the C-O bond distance. Upon going from hydrogen bonded to axial bonded to bridging ligands, the C-O bond distance increases from 1.200 to 1.250 to 1.303 (av.) Å. This is as expected, since the uncomplexed lactam should have a pure C-O double bond, whereas the complexed ligands show some conjugation.

It is of interest to compare the molecular structures of compounds (**1a**) and (**2a**) with the structure of the dirhodium(II)

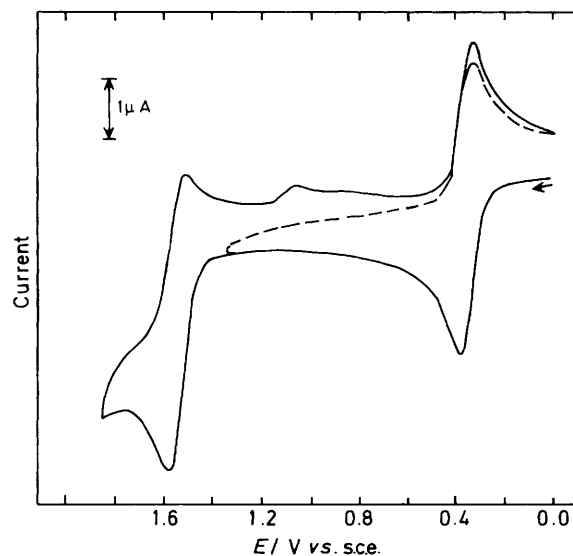


Figure 3. Cyclic voltammogram of $6 \times 10^{-4} \text{ mol dm}^{-3} [\text{Rh}_2(\text{pyro})_4]$ (**1**) in acetonitrile; $0.1 \text{ mol dm}^{-3} \text{NBu}_4\text{ClO}_4$. Scan rate, 100 mV s^{-1}

thiocaprolactamate complex,^{2a} $[\text{Rh}_2(\text{tcl})_4(\text{Htcl})]$ (**3**), and to evaluate the effect of substituting sulphur for oxygen in the bridging ligand. As stated earlier, a different geometric isomer is formed when the complex is synthesized by equatorial ligand exchange. Compound (**3**) forms an isomer in which one rhodium ion is bonded to four equatorial sulphur donors, and as a result the axial site on the rhodium bound to the four thiolactam nitrogens is sterically hindered to the point that the complex forms only mono axial adducts. The Rh-Rh bond distance for $[\text{Rh}_2(\text{tcl})_4(\text{Htcl})]$, 2.497 Å, is much longer than that found for (**1a**) or (**2a**), even though the latter two complexes have two axial ligands. The complex $[\text{Rh}_2(\text{SCOCH}_3)_4(\text{HSCOCH}_3)_2]$ also has a very long Rh-Rh bond distance of 2.55 Å.⁶ The longer metal-metal bond is due to the presence of a sulphur donor on the bridging ligand and probably results more from the size of the sulphur atom than from an electronic effect.

Cyclic Voltammetry of Complexes (1) and (2).—Cyclic voltammograms of (**1**) and (**2**), the axially unligated complexes $[\text{Rh}_2(\text{pyro})_4]$ and $[\text{Rh}_2(\text{vall})_4]$, are similar to the voltammograms of dirhodium complexes which have bridging ligands containing mixed N and O donor atoms such as $[\text{Rh}_2(\text{O}_2\text{CCH}_3)_n(\text{RNCOR}')_{4-n}]$.^{7,8} These types of complexes undergo two reversible metal-centred oxidations which are represented by equations (1) and (2).

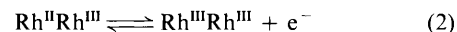
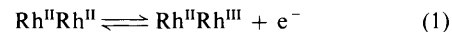


Table 4 lists potentials for the first and second oxidation of complexes (**1**) and (**2**) in three different solvents containing $0.1 \text{ mol dm}^{-3} \text{NBu}_4\text{ClO}_4$. Both compounds undergo two reversible one-electron oxidations (ΔE_p , ca. 60 mV) as illustrated by the cyclic voltammogram of (**1**) in acetonitrile (Figure 3). The potentials for the first oxidations vary with the bridging ligand and the solvent used. The first oxidation of (**1**) occurs at +0.15 V in acetonitrile and at +0.31 V in methylene chloride. The first oxidation of compound (**2**) occurs at +0.24 V in methylene chloride, +0.04 V in acetonitrile, and at +0.08 V in acetone. These values are consistent with the oxidation potentials of $[\text{Rh}_2(\text{O}_2\text{CCH}_3)_n(\text{RNCOR}')_{4-n}]$ in different solvent media.⁷

Table 4. Half-wave potentials for the first and second oxidations of compounds (1) and (2) in different solvents containing 0.1 mol dm⁻³ NBu₄CIO₄

Compound	Solvent	$E_{1/2}$ /V vs. s.c.e.	
		1st Oxidation	2nd Oxidation
(1)	CH ₂ Cl ₂ ^a	+0.31	+1.33
	CH ₃ CN	+0.15	+1.33
	Acetone ^a	≈ +0.13	<i>b</i>
(2)	CH ₂ Cl ₂	+0.24	+1.31
	CH ₃ CN	+0.04	+1.30
	Acetone	+0.08	<i>b</i>

^a Poor solubility. ^b Cannot be obtained due to the limited solvent window for oxidation.

Also, the potentials for reactions (1) and (2) of other dirhodium complexes shift by approximately the same magnitude upon changing the number of amidate bridging ligands in [Rh₂(O₂CCH₃)_n(RNCOR')_{4-n}]^{5,6}

The second oxidation of compound (1) is followed by a slow irreversible chemical reaction (the product of which was not characterized) but a small re-reduction peak appears at $E_p = +0.85$ V after scanning past the second oxidation. This is illustrated in Figure 3. A chemical reaction does not follow the second oxidation of compound (2), which in CH₃CN occurs at $E_{1/2} = +1.30$ V.

The potential for the second oxidation of (1) and (2) is not sensitive to solvent changes as is the case for the first oxidation. The second oxidation of compound (1) occurs at $E_{1/2} = +1.33$ V in both methylene chloride and acetonitrile. Compound (2) is oxidized at $E_{1/2} = +1.31$ V in methylene chloride and at +1.30 V in acetonitrile. These second oxidations are difficult to observe in acetone due to a decrease in the positive potential range of the solvent.

It should be pointed out that [Rh₂(HNCOCH₃)₄] has the same first oxidation potential as compound (1) in acetonitrile (+0.15 V) but that its second oxidation potential is nearly 100 mV more positive than that of (1).⁸ This difference combined with the insensitivity of the second oxidation towards the bridging and axial ligands suggests that the second oxidations of (1) and (2) involve a molecular orbital with significant bridging ligand character.

E.S.R. Spectra.—The electro-oxidation product of reaction (1) was investigated by e.s.r. spectroscopy and can be formally described as a dirhodium(II,III) species. The singly oxidized dirhodium species generated by controlled potential electrolysis are not e.s.r. active at room temperature in any of the investigated solvents. E.s.r. spectra are observed at low temperature, however. Figure 4 illustrates the frozen glass (< -150 °C) e.s.r. spectra of [Rh₂(vall)₄]⁺ (2⁺) obtained after the oxidation in CH₂Cl₂ and CH₃CN. Table 5 summarizes g values for the singly oxidized complexes (1⁺) and (2⁺) in different solvents.

The axial e.s.r. spectra ($g_{\perp} > g_{\parallel}$) of [Rh₂(pyro)₄]⁺ and [Rh₂(vall)₄]⁺ in both CH₂Cl₂ and CH₃CN are similar to those of [Rh₂(O₂CCH₃)_n(RNCOR')_{4-n}]⁺ in CH₃CN.⁸ The g_{\parallel} is split into a 1:2:1 triplet by two equivalent ¹⁰³Rh nuclei ($I = \frac{1}{2}$), indicative of a formal Rh^{II}Rh^{III} species where the unpaired electron is delocalized equally on both rhodium atoms. The g_{\perp} and g_{\parallel} values for complexes (1) and (2) are nearly identical in all three solvents and may be compared with the g values of [Rh₂(HNCOCH₃)₄] ($g_{\perp} = 2.11$ and $g_{\parallel} = 1.92$)⁷ and

Table 5. E.s.r. data of singly oxidized compounds (1⁺) and (2⁺)

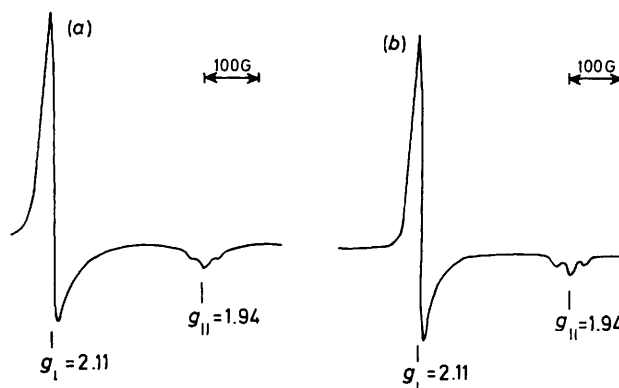
Solvent	(1 ⁺)		(2 ⁺)	
	g_{\perp}	g_{\parallel} *	g_{\perp}	g_{\parallel} *
CH ₂ Cl ₂	2.10	1.93	2.11	1.94
CH ₃ CN	2.10	1.94	2.11	1.94
Acetone			2.11	1.94

* g_{\parallel} is split into a 1:2:1 triplet in all three solvents.

Table 6. Peak maxima in the electronic absorption spectra of neutral and singly oxidized compounds (1) and (2)

Solvent	$\lambda_{\max.}/\text{nm}$ ($10^{-2} \epsilon/\text{dm}^3 \text{ mol}^{-1} \text{ cm}^{-1}$)			
	(1)	(1 ⁺)	(2)	(2 ⁺)
CH ₂ Cl ₂	626 ^a	ca. 485, ca. 520 ^b	664 (1.7)	503 (39)
CH ₃ CN	500 (2.3)	485 (45), 520 ^b	510 (2.5)	503 (51)
Acetone	565 ^a		604 (2.1)	489 (44)
Water	540 ^a		572 (2.0)	ca. 495

^a Poor solubility. ^b Unresolved broad peak.

**Figure 4.** E.s.r. spectra of singly oxidized [Rh₂(vall)₄]⁺ (2⁺) in (a) methylene chloride and (b) acetonitrile containing 0.1 mol dm⁻³ NBu₄CIO₄

[Rh₂(tcl)₄(Htcl)] ($g_{\perp} = 2.11$ and $g_{\parallel} = 2.02$).^{2a} The values and splitting of the g tensors are consistent with the odd electron orbital being δ^* and with the spin density being equally distributed over both rhodium atoms.⁹ However, since the unpaired electron is in a metal-centred orbital, it is not clear why the second oxidation potentials of (1) and (2) are not sensitive to solvent interactions similar to the case of the first oxidation. The value of g_{\parallel} for the two lactam complexes is less than g_{\perp} , whereas g_{\parallel} for the thiolactam is greater than g_{\perp} . Based on theoretical predictions⁸ the h.o.m.o. of the latter complex should be metal centred and have σ symmetry. Also, g_{\parallel} for (1) and (2) is split into a 1:2:1 triplet by the $\frac{1}{2}$ nuclear spin of the two rhodium atoms and (3) shows only a broad unresolved singlet for g_{\parallel} .^{2a}

Electronic Absorption Spectra.—Figure 5(a) and (b) show the electronic absorption spectra of neutral and singly oxidized (1) in acetonitrile while Figure 5(c) and (d) show the electronic absorption spectra of neutral and singly oxidized (2) in the same solvent. The absorption peak maxima and molar absorptivities of these species in four different solvent systems are summarized in Table 6.

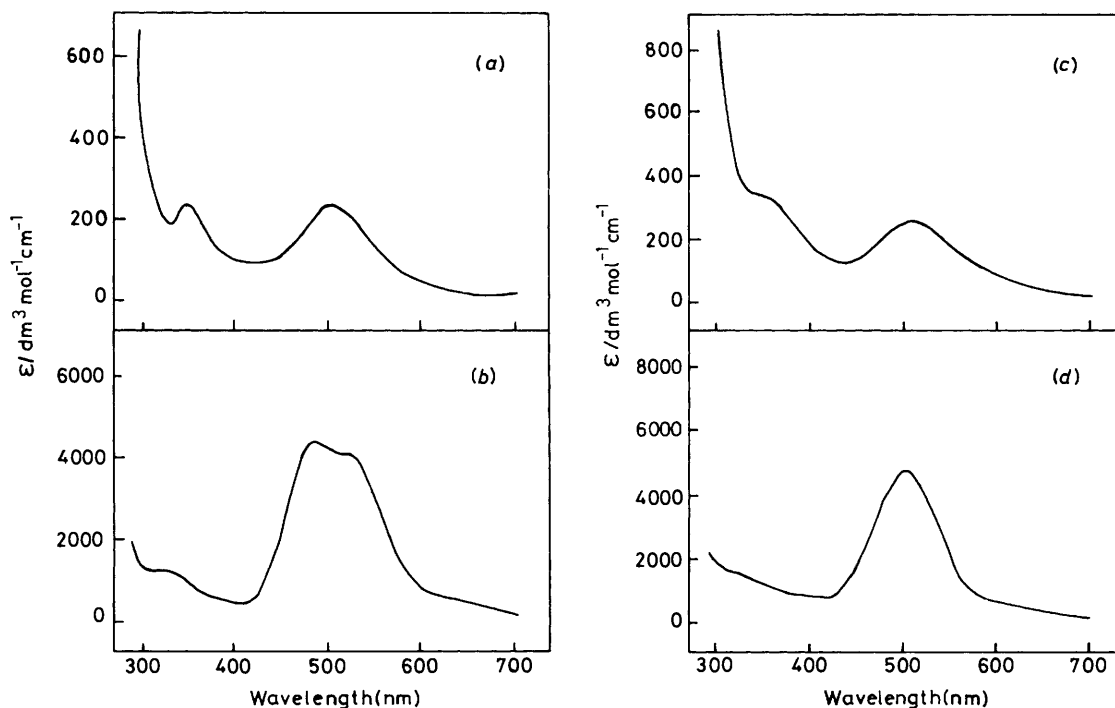


Figure 5. Electronic absorption spectra of (a) (1), (b) electrochemically generated, singly oxidized (1^+), (c) (2), and (d) electrochemically generated, singly oxidized (2^+) in acetonitrile

Neutral complexes (1) and (2) in acetonitrile have broad absorption bands at 500 and 510 nm, respectively. The wavelengths and the molar absorptivities of these complexes in acetonitrile are similar to those of $[\text{Rh}_2(\text{HNC}(\text{OCH}_3)_4)]$ in the same solvent system.⁸ The absorption band at ca. 500 nm shifts to longer wavelengths upon changing the solvent from acetonitrile to water, from water to acetone, and from acetone to methylene chloride. The same trend is observed for the shift of the lowest-energy absorbance band of $[\text{Rh}_2(\text{O}_2\text{CCH}_3)_4]$ and $[\text{Rh}_2(\text{HNC}(\text{OCH}_3)_4)]$ in these solvents.⁸ Based on theoretical and experimental results, the lowest energy absorbance of $[\text{Rh}_2(\text{O}_2\text{CCH}_3)_4]$ has been assigned to the Rh–Rh $\pi^* \rightarrow \text{Rh-Rh } \sigma^*$ transition.

The electro-oxidation of complexes (1) and (2) in methylene chloride or in acetonitrile gives rise to a species with high intensity absorption bands ($\epsilon \approx 4 \times 10^3 \text{ dm}^3 \text{ mol}^{-1} \text{ cm}^{-1}$) in the electronic absorption spectra. The singly oxidized form of (1) has a broad absorption which is comprised of two peaks at 485 and 520 nm. The relative intensities of these two peaks are only slightly affected by the solvent and identical wavelength maxima are observed for the singly oxidized complex (1^+) in acetonitrile and methylene chloride. This is surprising since there is a large difference ($4.03 \times 10^3 \text{ cm}^{-1}$) between wavelengths of the neutral complex (1) in these two solvents.

The singly oxidized complex (2^+) has a high intensity absorption at 503 nm in both methylene chloride and acetonitrile. The appearance of intense bands ($\epsilon > 10^3$) in the visible region after the first oxidation is characteristic of all dirhodium amidate complexes including $[\text{Rh}_2(\text{O}_2\text{CCH}_3)_3(\text{HNC}(\text{OCH}_3))]^+$ which has only one acetamidate bridging ligand.^{8,10} Thus this band (or bands) is related to the presence of the nitrogen donor and probably involves a ligand-to-metal charge transfer. The fact that the energy of this transition is the same for a given amidate complex in bonding and non-bonding solvents shows that a Rh–Rh orbital of σ symmetry is not involved.

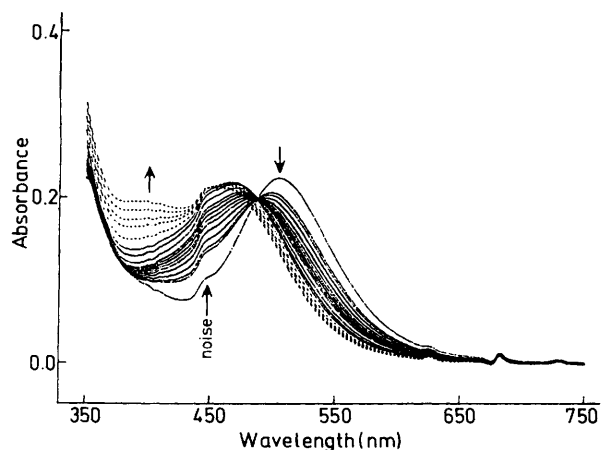


Figure 6. Changes in the electronic absorption spectrum of compound (1) in CH_3CN as a function of increasing partial pressure of CO; (—) 0 to 0.3 atm CO and (---) 0.44 to 1 atm CO

Reversible CO Binding by Compounds (1) and (2).—Dirhodium(II,II) complexes of the form $[\text{Rh}_2(\text{O}_2\text{CCH}_3)_n(\text{RNCOR}')_{4-n}]$ reversibly bind carbon monoxide¹ and this is also the case for complexes (1) and (2). Bubbling of CO through solutions of (1) and (2) generates the CO adduct(s) while dissociation of CO occurs upon bubbling pure nitrogen through the solution.

Figure 6 shows the changes which occur in the electronic absorption spectrum of complex (1) in CH_3CN as a function of increasing CO partial pressure. As the CO pressure is increased, a peak initially occurs at 465 nm and the peak at 500 nm decreases. An isosbestic point is observed at 485 nm. However, this isosbestic behaviour is lost at $p_{\text{CO}} > 0.1 \text{ atm}$ and no further

Table 7. Half-wave potentials for the first oxidation and CO binding constants of compounds (1), (2), and $[\text{Rh}_2(\text{O}_2\text{CCH}_3)_n(\text{HNCOCH}_3)_{4-n}]$ in CH_3CN ; $0.1 \text{ mol dm}^{-3} \text{NBu}_4\text{ClO}_4^a$

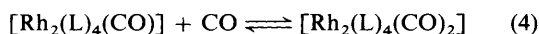
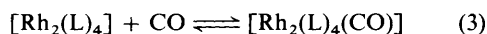
Compound	E_1/V vs. s.c.e.	$\log(K_{\text{CO}}/\text{atm}^{-1})^b$
(1)	0.15	1.63 ± 0.05
(2)	0.04	2.11 ± 0.06
$[\text{Rh}_2(\text{O}_2\text{CCH}_3)_4]$	1.17	No reaction
$[\text{Rh}_2(\text{O}_2\text{CCH}_3)_2(\text{HNCOCH}_3)_2]$	0.62	0.08 ± 0.01
$[\text{Rh}_2(\text{O}_2\text{CCH}_3)(\text{HNCOCH}_3)_3]$	0.37	0.68 ± 0.03
$[\text{Rh}_2(\text{HNCOCH}_3)_4]$	0.15	1.51 ± 0.05

^a Values for $[\text{Rh}_2(\text{O}_2\text{CCH}_3)_n(\text{HNCOCH}_3)_{4-n}]$ taken from refs. 1 and 6.

^b For CO binding according to equation (3).

isosbestic behaviour is seen up to a CO pressure of 0.3 atm. At CO pressures higher than 0.44 atm another isosbestic point is observed.

The above changes indicate that two equilibria are involved in the binding of CO. These equilibria are given by reactions (3) and (4) (where L = pyro or vall) which overlap in a range of CO pressure between 0.1 and 0.44 atm.



A method for calculating CO binding constants using the Ketelaar equation has been described in the literature.¹ Plots of $1/(A - A_0)$ vs. $1/p_{\text{CO}}$ give K_{CO} , but equilibrium constants by this method can only be calculated for reaction (3). The CO binding constants of complexes (1) and (2) were determined using the same method,¹ but with an improvement described in the Experimental section.

The CO binding constants for complexes (1) and (2) are too large to be accurately measured in either methylene chloride or 1,2-dichloroethane. However, values can be determined in CH_3CN . These values are listed in Table 7 which also lists half-wave potentials and CO binding constants of the other $[\text{Rh}_2(\text{O}_2\text{CCH}_3)_n(\text{RNCOR}')_{4-n}]$ complexes in acetonitrile.

Figure 7 shows the relationship between E_1 for reaction (1) and CO binding constants of the complexes listed in Table 7. It is clear that the data for complexes (1) and (2) in acetonitrile fit well with an earlier proposed correlation.¹ CO binding constants of $6.3 \times 10^3 \text{ atm}^{-1}$ and $1.2 \times 10^4 \text{ atm}^{-1}$ can be estimated for complexes (1) and (2) if a similar correlation also exists in 1,2-dichloroethane. The estimated K_{CO} value for compound (2) in dichloroethane is *ca.* 10^4 times greater than that reported for CO binding by $[\text{Rh}_2(\text{O}_2\text{CCH}_3)_4]$. The electrochemical and X-ray photoelectron spectroscopic studies on carboxylate and amidate complexes show that the rhodium core electrons^{2b} ($3d_3$) and the h.o.m.o. of the rhodium amidate complexes are *ca.* 0.1 V higher in energy than the corresponding carboxylate. Strong electron-donor bridging ligands have an overall charging effect on the metal centred orbitals. The increased radial extension of the filled Rh-Rh π orbitals makes the amidate complexes strong π donors with respect to CO bonding. The major difference between the ligand binding reactivity of compounds (1) and (2) and that of the thiolactam complex (3) is in the kinetic stability of the adducts of (3). Axial bonded lactams of (1) and (2) can be rapidly displaced by CO or other ligands but the mono thiolactam adduct of (3) is kinetically inert with ligands other than CO. Even with CO the axial exchange reaction for (3) is slow and shows second-order kinetics.^{2a}

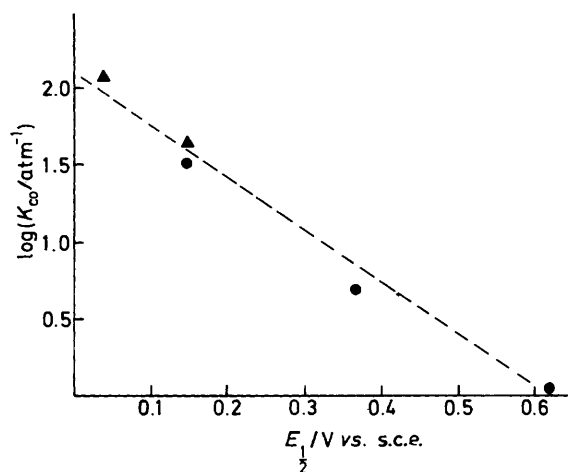


Figure 7. Correlation between CO binding constants and first oxidation potential of $[\text{Rh}_2(\text{O}_2\text{CCH}_3)_n(\text{HNCOCH}_3)_{4-n}]$ ($n = 0, 1, 2$) (●) and complexes (1) and (2) in acetonitrile (▲). Values of K_{CO} and E_1 are listed in Table 7

Most dirhodium(II) complexes undergo rapid exchange of axial ligands and in all these cases bis adducts are found. It is also well documented that formation of a second axial bond thermodynamically weakens the existing axial ligand interaction.¹¹ Therefore, the kinetic inertness of (3) with respect to (1) and (2) can be related to the inability of (3) to form a second axial bond. The cavity around the vacant axial site of (3) is small and only a molecule as small as CO can interact with the uncomplexed rhodium ion. This weak interaction with CO is apparently sufficient to labilize the *trans* axial ligand and thus show the second-order kinetics.

Conclusions

In conclusion, (1) and (2) have the same *cis* geometric arrangement of N and O donors as $[\text{Rh}_2(\text{HNCOCH}_3)_4]$.⁴ Therefore, the 'polar' arrangement of bridging ligands observed for (3) appears to be due to the presence of the sulphur donor and not to structural properties of the lactams. During the synthesis of (1), (2), and (3) it was observed that the rate of formation of the tetrasubstituted complex was much faster for ω -thiocaprolactam than for 2-pyrrolidinone or δ -valerolactam. It should also be mentioned that the five-membered ring lactam (2-pyrrolidinone) exchanges with acetate much faster than the six-membered ring lactam (δ -valerolactam). The fact that ω -thiocaprolactam, a seven-membered ring, exchanges faster than the two lactams implies that the presence of the sulphur donor labilizes the dirhodium(II) acetate bonds. Thus it would appear that the difference in bonding geometry between (3) and the two lactam complexes, (1) and (2), is controlled by electronic effects resulting from Rh-S bonding. However, the tetrakis(thioacetate) complex, $[\text{Rh}_2(\text{SOCCH}_3)_4]$, has the same *cis* arrangement of heterodonor as (1) and (2). This suggests that the presence of S donors alone does not dictate a particular geometric isomer being formed.

The electronic absorption spectra of the oxidized and reduced forms of (1) and (2), as well as e.s.r. spectra of the oxidized forms, are similar to spectra observed for neutral and oxidized $[\text{Rh}_2(\text{HNCOCH}_3)_4]$. The CO binding constants are larger for (1) and (2) than for $[\text{Rh}_2(\text{HNCOCH}_3)_4]$ and are in the order (2) > (1) > $[\text{Rh}_2(\text{HNCOCH}_3)_4]$. A good correlation exists between CO binding constants and the first oxidation potential of these complexes, *i.e.* the CO binding energy increases as the energy of the metal centred orbitals increases. The major

difference in the chemistry of (1) and (2) with respect to that of (3) is in the kinetic inertness of the Rh-axial ligand bond for (3). This appears to be due to the fact that (3) forms only mono adducts both in the solid state and in solution.

Acknowledgements

This work was supported by the Robert Welch Foundation (K. M. K. Grant No. E-680 and J. L. B. Grant No. E-918).

References

- 1 M. Y. Chavan, M. Q. Ahsan, R. S. Lifsey, J. L. Bear, and K. M. Kadish, *Inorg. Chem.*, 1986, **25**, 3218.
- 2 (a) R. S. Lifsey, M. Y. Chavan, L. K. Chau, M. Q. Ahsan, K. M. Kadish, and J. L. Bear, *Inorg. Chem.*, 1987, **26**, 822; (b) M. Q. Ahsan, I. Bernal, and J. L. Bear, *ibid.*, 1986, **25**, 260.
- 3 A. M. Dennis, J. D. Korp, I. Bernal, R. A. Howard, and J. L. Bear, *Inorg. Chem.*, 1983, **22**, 1522.
- 4 M. Y. Chavan, X. Q. Lin, M. Q. Ahsan, I. Bernal, J. L. Bear, and K. M. Kadish, *Inorg. Chem.*, 1986, **25**, 1281.
- 5 R. S. Lifsey, X. Q. Lin, M. Y. Chavan, M. Q. Ahsan, K. M. Kadish, and J. L. Bear, *Inorg. Chem.*, 1987, **26**, 830.
- 6 L. M. Dikareva, G. G. Sadikov, M. A. Parai-Koshits, M. A. Golubnichaya, I. B. Baranovskii, and R. M. Shchelokov, *Russ. J. Inorg. Chem.*, 1977, **22**, 1093.
- 7 T. P. Zhu, M. Q. Ahsan, T. Malinski, A. M. Dennis, K. M. Kadish, and J. L. Bear, *Inorg. Chem.*, 1984, **23**, 2.
- 8 M. Y. Chavan, T. P. Zhu, X. Q. Lin, M. Q. Ahsan, J. L. Bear, and K. M. Kadish, *Inorg. Chem.*, 1984, **23**, 4538.
- 9 T. Kawamura, H. Katayama, and T. Yamabe, *Chem. Phys. Lett.*, 1986, **130**, 20.
- 10 J. L. Bear, T. P. Zhu, T. Malinski, A. M. Dennis, and K. M. Kadish, *Inorg. Chem.*, 1984, **23**, 674.
- 11 T. R. Felthouse, *Prog. Inorg. Chem.*, 1982, **29**, 73 and refs. therein.

Received 9th November 1987; Paper 7/1979